Techniques, John Wiley, New York (1977).
Russell, T. W. F., and D. T. Buzzelli, "Reactor Analysis and Process Synthesis for a Class of Complex Reactions," *Ind. Eng. Chem. Proc. Des. Dev.*, **5**, 2 (1969).
Spendley, W., G. R. Hex, and F. R. Himsworth, "Sequential Applications of Simplex Designs in Optimization and Evolutionary Operation," *Technometrics*, **4**, 441 (1962).
Umeda, T., and A. Ichikawa, "a Modified Complex Method for Optimization," *Ind. Eng. Chem. Proc. Des. Dev.*, **10**, 236 (1971).
Van de Vusse, J. G., "Plug-Flow Type Reactor versus Tank Reactor," *Chem. Eng. Sci.*, **19**, 994 (1969).
Wegstein, J. H., "Accelerating Convergence of Iterative Process," *Comm. Assoc. Computing Machinery*, **1**, 9 (1958).

Manuscript received February 16, and accepted October 20, 1983.

Gas-Liquid Mass Transfer in Fluidized Particle Beds

Gas/liquid mass transfer has been studied in air/water fluidized beds of 0.05–8 mm glass spheres in a 0.14 m diameter reactor. The volumetric mass transfer coefficients k_La were independent of bed height, and, for particle diameters up to 1 mm, decreased linearly with solids concentration. Low solids loadings as well as large diameter particles significantly increased k_L and a, respectively, as compared to the two-phase system.

K. NGUYEN-TIEN,
A. N. PATWARI,
A. SCHUMPE,
and W.-D. DECKWER

Fachbereich Chemie—Technische Chemie
Universität Oldenburg
Oldenburg, West Germany

SCOPE

In gas-liquid fluidization, a particle bed is fluidized by cocurrent upwards gas and liquid flows. Small particles can also be fluidized by gas-induced liquid motion alone in a bubble column slurry reactor. Applications of three-phase bubble column reactors are numerous including catalytic hydrogenations and oxidations, synthesis gas conversion processes, and coal liquefaction. Usually, mass transfer can be modelled by the concept of resistances in series: i.e., gas-liquid and liquid-solid mass transfer and the chemical reaction at the solid surface are noninteracting steps. Nevertheless, the presence of the solids hydrodynamically affects the gas-liquid mass transfer. Since this transfer step may considerably contribute to the overall resistance, solids effects on the volumetric mass transfer coefficients k_La are an important information for the design of three-phase reactor.

Previous studies concentrated on large particle diameters. Glass spheres of about 1 mm diameter were found to decrease oxygen-water mass transfer, whereas at diameters exceeding 3 mm, k_La significantly increased as compared to the air/water system. Confusing results on axial variation of k_La and on effects of liquid flow rates have been reported that may partly refer to inadequate experimental design and modelling.

It is the objective of this study to provide reliable data for the solids effects on gas-liquid mass transfer in a wide range of particle diameters (0.05–8 mm) and gas and liquid superficial velocities. The measurements were carried out in a 0.14 m diameter reactor and air/water fluidized beds of 0.38–2.65 m height. Volumetric mass transfer coefficients were determined from the steady-state axial profiles of the oxygen liquid-phase concentration accounting for dispersion in the liquid phase. Emphasis was laid on the effects of small-sized particles because of their greater range of application in industry and the lack of reported data.

CONCLUSIONS AND SIGNIFICANCE

The volumetric gas-liquid mass transfer coefficients k_La were independent of the bed height and the axial position within the bed. At same liquid flow rate, k_La ran through a minimum with increasing particle size. Spheres of diameters exceeding 3 mm increased the gas-liquid mass transfer by factors up to 4 at low gas velocities. Most previously reported results agreed reasonably under these conditions. At high gas velocities the bubble disintegration effect of the particles was less pronounced, thus rendering the process energetically inefficient.

It was observed that in the case of small particles the effect of the particle diameter and the influence of the liquid flow variations can be combined into one characteristic factor which is the solids fraction ϕ_S in the suspension. The volumetric mass transfer coefficients in the presence of small fluidized particles were found to be merely a linear function of the solids fraction in the suspension. Comprehensive data for four different particle diameters from 0.05 to 1 mm at five different liquid flow rates and superficial gas velocities of 0.02 to 0.16 $m \cdot s^{-1}$ were empirically correlated by the relation:

$$k_La''' = 0.39\left(1 - \frac{\bar{\phi}_S}{0.58}\right)\bar{u}_G^{0.67}$$

(s^{-1}) $(m \cdot s^{-1})$

Correspondence concerning this paper should be addressed to W.-D. Deckwer.

with 11% mean deviation. At low gas velocities and low solids loadings, specifically,

$$\phi_S < (0.58 - 0.70\ \bar{u}_C^{0.15}) \quad \text{(m/s)}$$

the solids significantly increased gas-liquid mass transfer, presumably, by increasing the liquid-side mass transfer coefficients k_L. Further studies are needed to access the effects of particle shape and density and different liquid properties.

INTRODUCTION

Recently, three-phase fluidization was reviewed by Epstein (1981) emphasizing the fundamental aspects of fluid dynamics and pointing out present knowledge gaps. Among the various kinds of three-phase fluidization, gas-liquid fluidization appears to be the most important operation mode. Here, a particle bed is fluidized by cocurrent upwards gas and liquid flows. Although only a few applications of three-phase fluidized beds with larger particles can be found in chemical process industry, the majority of work published hitherto concerns gas-liquid fluidization of larger particles, i.e, $d_s > 1$ mm.

An important step in the overall performance of gas-liquid fluidized beds as chemical reactors is gas-liquid interphase mass transfer. A number of investigations on gas-liquid mass transfer in fluidized particle beds have already been published. Dhanuka and Stepanek (1980) recently reviewed all relevant results published until 1980. Though the general trends reported in the various studies are similar, quantitative agreement is often poor. Therefore, Dhanuka and Stepanek express doubt about the correctness of the available mass transfer data. We feel, however, that the confusion about the reliability of the available volumetric mass transfer coefficients (k_La) can be attributed to one or several of the following reasons:

- k_La was determined from one-point measurements instead of evaluating profiles measured along the particle bed. Thus, confusing dependencies on bed height have been found (Lee and Worthington, 1974; Østergaard and Suchozebrski, 1968; Østergaard and Fosbøl, 1972).
- Use of inappropriate models which, for instance, neglect liquid-phase dispersion and pressure variation. Hence, the driving concentration difference is not clearly defined (Dakshinamurty et al., 1974).
- Application of chemical methods in tall reactors in which small bubbles will be completely exhausted from gaseous reactant (Østergaard, 1978). Therefore, k_La data will be evaluated which are considerably too small.
- The experimental setup is not representative for industrial application (Dakshinamurty et al., 1974; Dhanuka and Stepanek, 1980; Alvarez-Cuenza and Nerenberg, 1981). In particular, the diameter of the particle bed is not large enough. In this case, the data may be falsified by the enlarged bed porosity at the wall. Such data are not reliable for scaling-up purposes.

The objective of this paper is to report on new gas-liquid mass transfer data in gas-liquid fluidized beds which were obtained by avoiding the misleading and detrimental effects mentioned above. Therefore, concentration profiles along the particle bed were measured, and these profiles were evaluated on the basis of appropriate models. It is, therefore, believed that the present data are particularly reliable. The experimental investigations cover a wide range of particle sizes and extend up to gas velocities of 0.16 m·s^{-1}. In addition, the diameter of the reactor can be assumed to be large enough to exclude significant wall effects.

EXPERIMENTAL

The experiments were carried out in a bubble column of 14 cm inner diameter and 265 cm height. The column was equipped with a conical bottom, the liquid entering at the center and the air being sparged through a ring distributor with 29 holes of 1 mm diameter. At the top of the cocurrently operated column, the walls extended into a wire screen retaining the solids. (Only the 0.05 mm glass spheres were recycled with the liquid.) The liquid overflowed into a nitrogen-sparged regeneration column and was recycled through a storage tank equipped with cooling coils. Gas-free liquid samples could be continuously withdrawn from the liquid inlet stream as well as from any one of ten tappings along the length of the column. The oxygen concentrations in the samples were measured with an oxygen electrode (Orion Research) in a stirred cell. The experimental arrangement has been described previously (Deckwer et al., 1982); details are reported elsewhere (Nguyen-tien, 1984). Glass spheres of diameters from 0.05 to 8.0 mm were applied. Experimental conditions are listed in Table 1.

ANALYSIS

Holdups

Phase holdups were determined from the measured static head profiles by solving the following equations:

$$\frac{-dP}{dl} = (\epsilon_G'''\rho_G + \epsilon_L'''\rho_L + \epsilon_S\rho_S)g \tag{1}$$

$$1 = \epsilon_G''' + \epsilon_L''' + \epsilon_S, \tag{2}$$

where $(\epsilon_G'''\rho_G)$ could be neglected in Eq. 1. The solids holdup ϵ_S was calculated from the known total mass of solids and the bed height H_S:

$$\epsilon_S = 4m_S/\rho_S H_S \pi D_C^2 \tag{3}$$

Particle entrainment caused visual observations of the bed height to be unreliable at $d_S < 3$ mm. Therefore, H_S was determined from the intercept of the linear portions of the pressure profiles in the two- and the three-phase zones. In case of the 0.05 mm diameter spheres, ϵ_S was determined by gravimetric analysis of samples withdrawn from the column.

Volumetric Mass Transfer Coefficients

The axial profiles of the liquid-phase oxygen concentration at steady state were analyzed for the volumetric mass transfer coefficients k_La''' assuming a constant oxygen mole fraction in the gas phase and accounting for linear pressure profiles in the three- and the two-phase zones. Three different models were tested:

- Plug flow model (PFM)
- Axial dispersion model (ADM)
- Backflow cell model (BFCM).

TABLE 1. RANGES OF EXPERIMENTAL CONDITIONS ($\bar{u}_G$: 0.018–0.163 m·s^{-1}, T = 293 K)

d_S mm	$10^{-3}\ \rho_S$ kg·m^{-3}	$10^2\ u_{L,mf}$* m·s^{-1}	$10^2\ u_L$ m·s^{-1}	ϕ_S	H_S m
0.05	2.77	—	5.4–7.7	0.005–0.026	2.65
0.3	2.95	0.1	4.6–9.3	0.09–0.27	0.50–2.65
0.5	2.82	0.3	5.4–10.8	0.07–0.23	0.38–2.60
1.0	2.68	0.9	7.7–10.8	0.20–0.29	0.83–2.65
3.0	2.55	3.3	7.7–10.8	0.30–0.40	0.62–2.49
5.0	2.54	4.9	7.7–11.6	0.33–0.42	1.33–2.50
8.0	2.51	6.6	7.7–11.6	0.39–0.53	0.49–2.00

* Calculated from correlation suggested by Wen and Yu (1966).

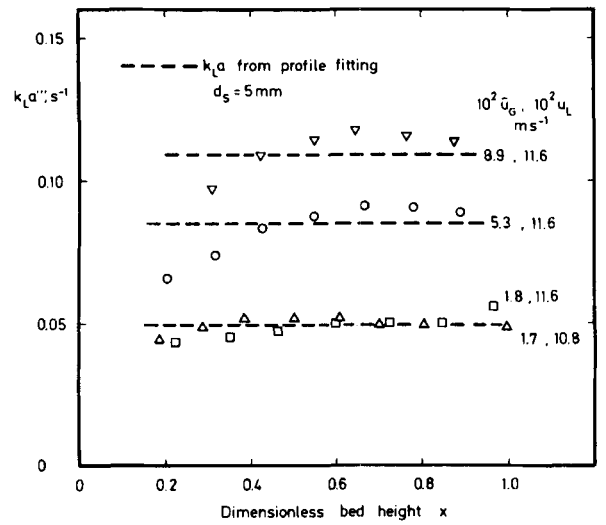

Figure 1. Axial variation of volumetric mass transfer coefficients from plug flow model.

For plug flow of the liquid (PFM) the oxygen mass balance for the liquid phase is:

$$-u_L \frac{dc}{dl} + k_L a'''(c^* - c) = 0 \tag{4}$$

Introducing

$$x = l/H_S \tag{5}$$

$$St''' = k_L a''' H_S/u_L \tag{6}$$

$$c^* = yP/He = yP_{TS}(1 + \alpha'''[1 - x])/He \tag{7}$$

where

$$P_{TS} = P_T(1 + \alpha'') \tag{8}$$

$$\alpha'' = \epsilon_L'' \rho_L g(L - H_S)/P_T \tag{9}$$

$$\alpha''' = (\epsilon_L''' \rho_L + \epsilon_S \rho_S) g H_S/P_{TS} \tag{10}$$

one obtains:

$$-\frac{dc}{dx} + St''' \left\{ \frac{yP_{TS}}{He}(1 + \alpha'''[1 - x]) - c \right\} = 0 \tag{11}$$

Integration results in:

$c = c_o e^{-St''' x}$

$$-\frac{yP_{TS}\alpha'''}{He}\left[x - \left(1 + \frac{1}{\alpha'''} + \frac{1}{St'''}\right)(1 - e^{-St''' x})\right] \tag{12}$$

Plug flow has been assumed by most previous investigators. Some of them reported pronounced axial profiles of the volumetric mass transfer coefficients k_La''' (Alvarez-Cuenza and Nerenberg, 1981; Lee and Worthington, 1974; Østergaard and Suchozebrski, 1968; Østergaard and Fosbøl, 1972). Partly, this has to be attributed to nonnegligibility of liquid-phase dispersion. Then, the concentration jump at the inlet causes the PFM to result in a decrease of k_La''' with increasing height. However, also for beds of larger particles where the assumption of plug flow is justified, pronounced maxima of k_La''' have been reported. Therefore, the PFM was again applied in this work. Axial variations of k_La''' were investigated by introducing individual local oxygen concentrations into Eq. 12; overall mean k_La''' values were obtained by fitting Eq. 12 to the full profiles in the three-phase zone. Typical results are depicted in Figure 1. Only in the lower zone some axial variation was observed but the overall deviation from the mean k_La''' was marginal. The volumetric mass transfer coefficients reported in this study are representative of the whole bed rather than local values.

The axial dispersion model (ADM) as described by Deckwer et al. (1982) could be applied only if $H_S \approx L$. If this condition was fulfilled, the results were in agreement with the generally applicable backflow cell model (BFCM).

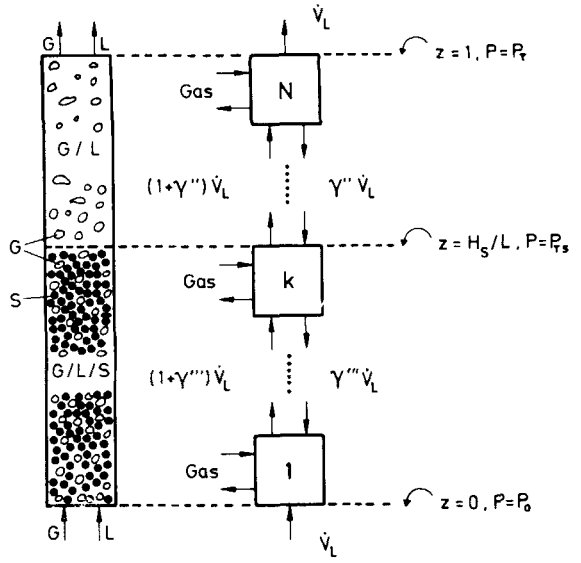

Figure 2. Schematic illustration of liquid-phase backflow cell model.

The BFCM is schematically illustrated in Figure 2. The bubble column modelled consists of N ideally mixed cells; liquid-phase dispersion was accounted for by liquid backflow between the cells. A value of $N = 27$ was chosen to allow sufficiently close simulation of plug flow conditions with zero backflow rate and to have all the sampling ports located at cell middles. The oxygen mass balances for the N cells are:

$j = N$

$$(1 + \gamma'')c_{N-1} - (1 + \gamma'')c_N + \frac{St''}{N - k}\left(\frac{yP_N}{He} - c_N\right) = 0 \tag{13}$$

$N > j > k$

$$(1 + \gamma'')c_{j-1} - (1 + 2\gamma'')c_j + \gamma'' c_{j+1} + \frac{St''}{N - k}\left(\frac{yP_j}{He} - c_j\right) = 0 \tag{14}$$

$j = k$

$$(1 + \gamma''')c_{k-1} - (1 + \gamma'' + \gamma''')c_k + \gamma'' c_{k+1} + \frac{St'''}{k}\left(\frac{yP_k}{He} - c_k\right) = 0 \tag{15}$$

$k > j > 1$

$$(1 + \gamma''')c_{j-1} - (1 + 2\gamma''')c_j + \gamma''' c_{j+1} + \frac{St'''}{k}\left(\frac{yP_j}{He} - c_j\right) = 0 \tag{16}$$

$j = 1$

$$c_o - (1 + \gamma''')c_1 + \gamma''' c_2 + \frac{St'''}{k}\left(\frac{yP_1}{He} - c_1\right) = 0 \tag{17}$$

where

$$St'' = \frac{k_L a''(L - H_s)}{u_L} \tag{18}$$

and the pressures in the cells are given by:

$j > k$

$$P_j = P_T\left(1 + \alpha''\left[1 - \frac{j - k - 0.5}{N - k}\right]\right) \tag{19}$$

$j \leq k$

$$P_j = P_{TS}\left(1 + \alpha'''\left[1 - \frac{j - 0.5}{k}\right]\right) \tag{20}$$

The backflow ratios are related to the liquid-phase Peclet numbers by:

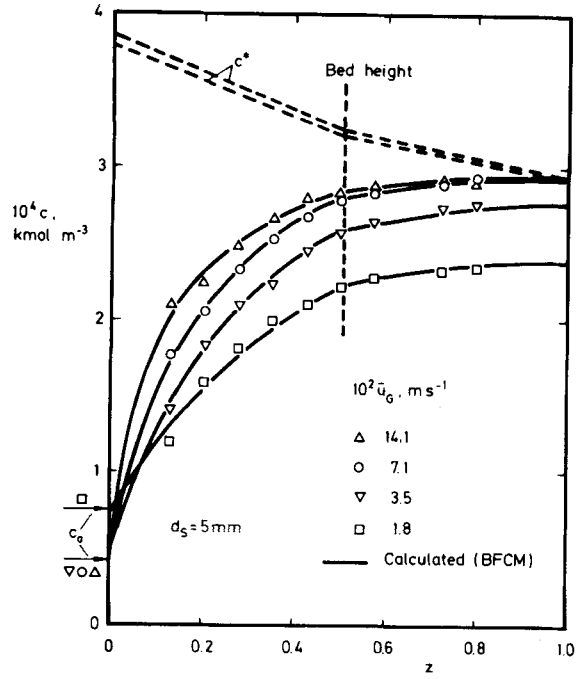

Figure 3. Fit of experimental oxygen liquid-phase profiles by BFCM.

$$\gamma'' = \frac{N-k}{Pe_L''} - 0.5 \tag{21}$$

$$\gamma''' = \frac{k}{Pe_L'''} - 0.5 \tag{22}$$

where

$$\widetilde{Pe_L''} = \frac{(L-H_S)u_L}{E_L''\epsilon_L''} \tag{23}$$

$$Pe_L''' = \frac{H_S u_L}{E_L'''\epsilon_L'''} \tag{24}$$

Equations 13 to 17 were solved and fitted to the experimental profiles by the methods of Thomas and Marquardt. Usually, only k_La''' and E_L''' were optimized whereas the two-phase zone was characterized by relations valid for bubble columns:

$$k_La'' = 0.467\,\bar{u}_G^{0.82} \tag{25}$$

(s^{-1}) $\quad$ $(m \cdot s^{-1})$

and

$$E_L'' = 0.68\,D_c^{1.4}\,\bar{u}_G^{0.3} \tag{26}$$

$(m^2 \cdot s^{-1})$ $\quad$ (m) $(m \cdot s^{-1})$

according to Shah et al. (1982) and Deckwer et al. (1974), respectively. Some typical profiles and their excellent fit by the BFCM are shown in Figure 3. The choice of k_La'' and E_L''' had very little influence on the results obtained for the three-phase zone because of the comparatively low driving force in the upper part of the column and, for larger particles, low dispersion in the three-phase zone. Tentatively also the parameters for the two-phase zone were optimized for some experiments with small H_S. The deviations from k_La in the solids-free column were relatively small (Figure 4). Thus, while bubble characteristics immediately above the bed have been reported to be strongly dependent on the size of the solid particles (Lee et al., 1974), with water as the liquid phase, coalescence and breakup gradually establish the usual two-phase characteristics.

For larger particles, the optimized dispersion coefficients E_L''' often reached the lower limit determined by the selected number of cells (usually, $N = 27$). Then, approaching plug flow of the liquid phase, the mass transfer coefficients obtained from the BFCM and the PFM were in agreement. With regard to the fit of the experimental profiles by means of the BFCM, the same conclusions as

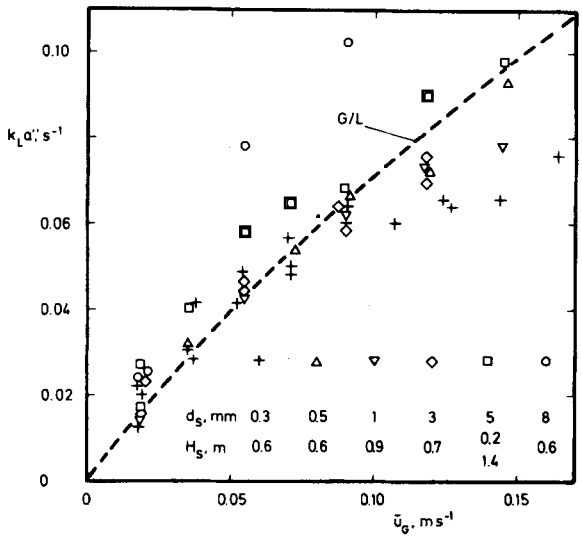

Figure 4. Volumetric mass transfer coefficients in the two-phase zone over three-phase fluidized beds.

drawn recently for the use of the ADM (Deckwer et al., 1984) are valid; i.e., the profile description is very sensitive to k_La''' variations but rather insensitive to changes in $\gamma'''(E_L''')$. However, this does not mean that dispersion in the liquid phase can generally be neglected as the concentration jump at reactor inlet can only be taken into account properly by application of a model which involves liquid-phase dispersion. The method employed here—fitting of steady-state profiles to the predictions of the BFCM—gives reliable k_La''' values, while the dispersion parameter (γ''', E_L''') is subject to considerable scatter (Deckwer et al., 1983). The dispersion parameters are reported elsewhere (Nguyen-tien et al., 1984). The volumetric mass transfer coefficients discussed in the following chapter were all evaluated with the BFCM.

RESULTS AND DISCUSSION

Hydrodynamics

As the solids holdups in the three-phase zone progressively increased with increasing particle diameter d_S, the gas holdups ran through a minimum at d_S of 1–3 mm. For smaller and larger particles, the gas holdups were relatively close to the two-phase (G/L) data. Except for low gas velocities, the bed heights and solids holdups correspondingly were almost independent of u_G. Initially, on introduction of the gas, the liquid fluidized beds expanded if $d_S > 3$ mm, and contracted if $d_S < 3$ mm. Contraction was about 50% for 0.3 mm spheres. This well known phenomenon results from diversion of part of the liquid flow into the solids-deficient wakes behind the gas bubbles (Epstein, 1981). Details on the hydrodynamic results are reported by Nguyen-tien (1984).

Mass Transfer

Gas/liquid mass transfer was studied with various amounts of solids, i.e., at different heights H_S of the three-phase zone. Contrary to the results reported by previous investigators (Lee and Worthington, 1974; Østergaard and Føsbol, 1972), there was no effect of bed height on the mass transfer coefficients k_La''' in the three-phase zone. Some typical results for different particle sizes are shown in Figure 5. Therefore, mass transfer data are reported without the need to distinguish with respect to bed height. For comparison, the two-phase (G/L) data are also indicated in the following figures. k_La for the air/water system was found to be practically independent of liquid velocityy ($u_L = 0.054 - 0.108$ m·s^{-1}) and is very well represented by Eq. 25.

The mass transfer coefficients k_La''' in the three-phase systems

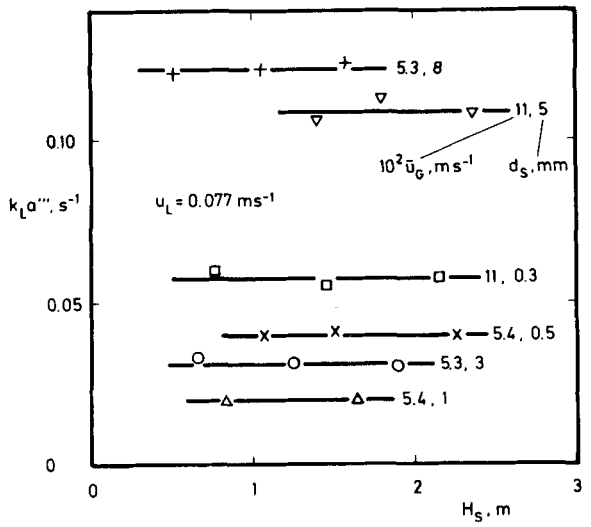

Figure 5. Dependence of volumetric mass transfer coefficients on bed height.

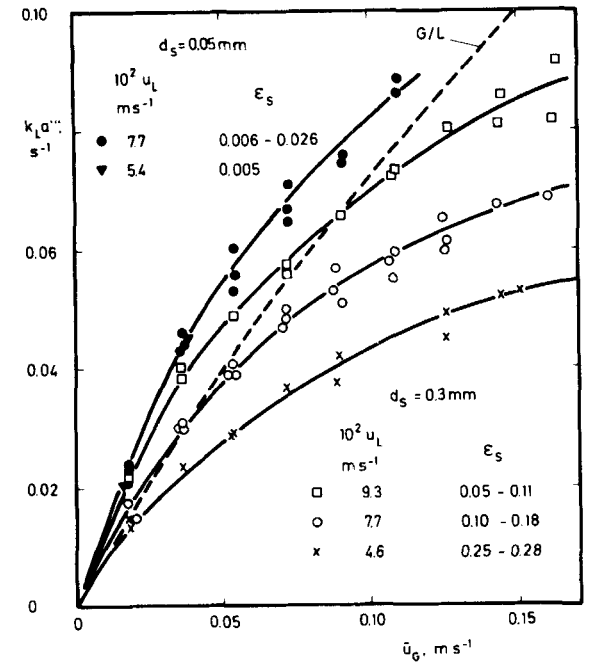

Figure 6. Effect of gas and liquid velocity on $k_L a'''$ in fluidized beds of 0.05 and 0.3 mm glass spheres.

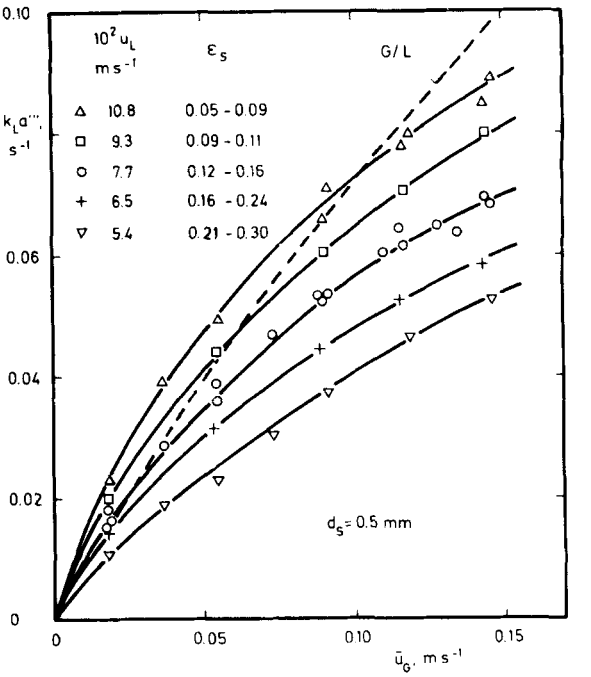

Figure 7. Effect of gas and liquid velocity on $k_L a'''$ in fluidized beds of 0.5 mm glass spheres.

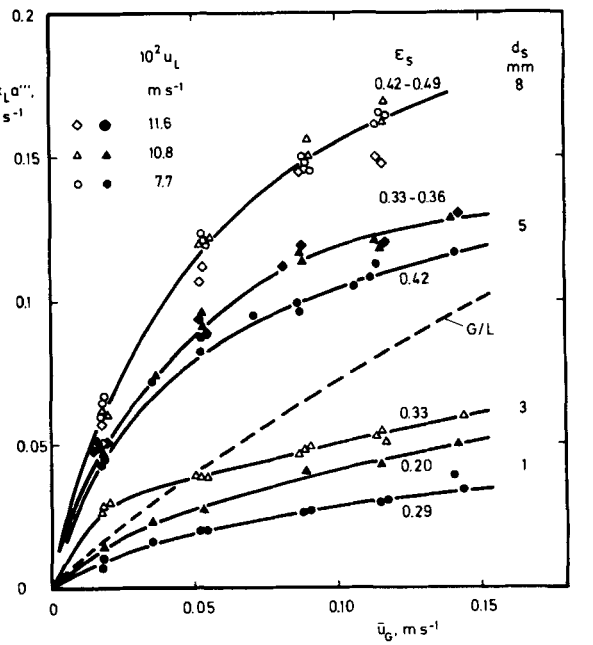

Figure 8. Volumetric mass transfer coefficients in fluidized beds of 1-8 mm diameter glass spheres.

are plotted against the gas velocity in Figures 6, 7 and 8. For the 0.05 mm particles slurries (Figure 6), $k_L a'''$ was significantly higher than in the two-phase (G/L) system. The relative increase was high, specially at low gas velocities. Since the gas holdups were uneffected, it may be speculated that the particles increased the liquid-side mass transfer coefficients k_L by penetrating the liquid-side diffusion film rather than affecting the specific interfacial area a. Quicker et al. (1983) applied the sulfite oxidation method to measure gas/liquid specific interfacial areas in slurries of fine particles (activated carbon, kieselguhr, and aluminium oxide with $d_S < 2 \times 10^{-5}$ m). No significant effects were observed at low solids loadings. At higher solids concentrations, a strong decrease of interfacial area occurred that could be correlated by the increased effective viscosities of the slurries. Such a decrease of interfacial area due to coalescence-promoting effect of higher solids holdup probably caused the decrease of volumetric mass transfer coefficient in beds of 0.3 mm glass spheres. Any increase of k_L by the solids was overcompensated by a decrease in a. Only at the highest applied liquid velocity and low gas velocities, $k_L a'''$ was still higher than in the two-phase system. Decreasing u_L and correspondingly increasing ϵ_S caused a reduction in gas/liquid mass transfer (Figure 6). (Additional data for 0.3 mm spheres at an intermediate liquid velocity of 0.054 m·s^{-1} are not shown for clarity.)

Same trends were observed for 0.5 mm glass spheres (Figure 7) at five different liquid velocities from 0.054 to 0.108 m·s^{-1}. Increase in particle diameter to 1 mm further increased ϵ_S at same liquid velocity and decreased $k_L a'''$ (Figure 8). However, for 3 mm glass spheres, the mass transfer coefficients were slightly higher; applying 5 and 8 mm spheres, $k_L a'''$ increased beyond the two-phase $k_L a$ though ϵ_S progressively increased. For 8 mm particles the ratio $k_L a'''/k_L a''$ decreased from about 4 at low gas velocity

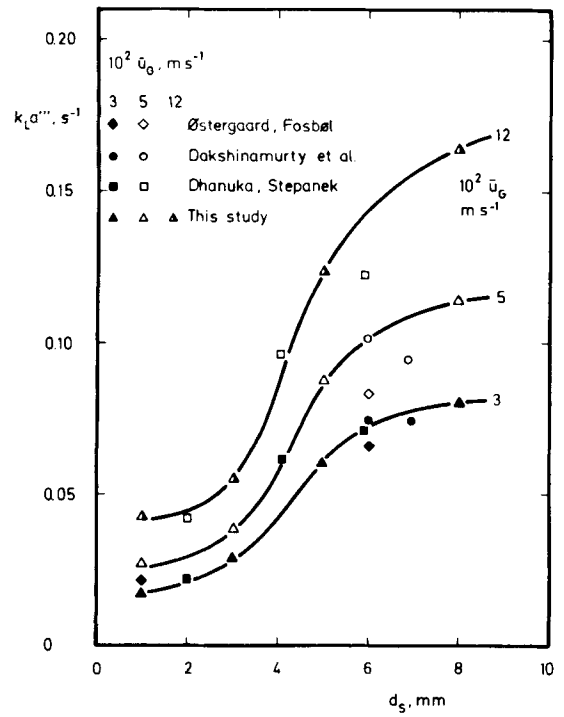

Figure 9. Comparison of published data on k_La''' in fluidized beds of 1–8 mm glass spheres ($u_L \approx 0.1$ m·s^{-1}).

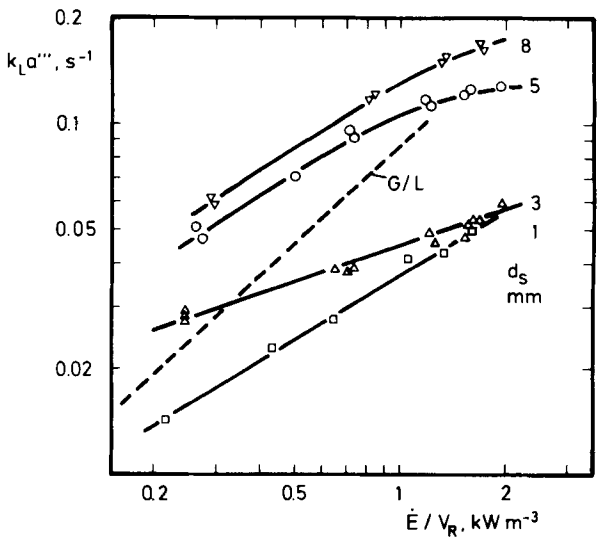

Figure 10. Energetic effectiveness of gas/liquid mass transfer in three-phase fluidized beds ($u_L = 0.108$ m·s^{-1}).

to about 2 at high gas velocity without significant effects of the applied liquid velocities (u_L = 0.077–0.116 m·s^{-1}).

A comparison with previous investigations employing large diameter particles is given in Figure 9. The literature data are restricted to low gas velocities where agreement with the present results is fairly good. The results of Dhanuka and Stepanek (1980) are high, probably, because of the addition of 1 M sodium carbonate/sodium bicarbonate for simultaneous determination of interfacial areas by chemical absorption of CO_2. The liquid-side mass transfer coefficients k_L evaluated by Dhanuka and Stepanek were similar in beds of different size glass spheres (2, 4 and 6 mm) whereas the interfacial areas strongly increased with increasing d_S. In this study, the gas holdups ϵ_G''' were about the two-phase ϵ_G for the particle diameters of 5 and 8 mm. Therefore, the strong increase in k_La''' and a''' has to be attributed to a decrease in bubble size by the solids. Two phenomena have been suggested as an explanation of bubble disintegration by large diameter solids:

- Penetration of bubbles by particles if Weber number > 3 (Lee et al., 1974).
- Rayleigh-Taylor instability of the bubble roofs (Henriksen and Østergaard, 1974).

Which of these phenomena is responsible for bubble disintegration in beds of large diameter particles is still under discussion (Epstein, 1981).

Although the phenomenon of bubble disintegration has often been studied, the energetic efficiency of three-phase fluidization has not been considered. The energy input consists of the energy required for compression of the gas and the kinetic energies of the gas and the liquid. The volume-specific energy input is:

$$\dot{E}/V_R = \frac{1}{V_R}\left(\dot{N}_G RT \ln\frac{P_o}{P_T} + \frac{\dot{m}_G}{2}u_{G,o}^2 + \frac{\dot{m}_L}{2}u_{L,o}^2\right) \quad (27)$$

As compared to the two-phase system, the first and the last term are higher due to the increased hydrostatic head and the high liquid flow rates required for fluidization, respectively. For this experiments, the kinetic energy of the liquid is of negligible magnitude as compared to the other terms. Therefore, increasing k_La''' by high liquid flow rates were generally advisable. The kinetic energy of the gas at a certain mass flow rate is determined by the size and the number of the gas distributor holes. The mass transfer characteristics, however, are certainly independent of the hole diameter in case of three-phase fluidized beds. Thus, it is merely the energy for compression due to hydrostatic head that has to be considered. Although V_R is proportional to bed height H_S whereas ($ln\ P_o/P_T$) increases underproportionally with H_S, the higher mass flow rates required for same mean superficial gas velocity compensate for this almost quantitatively; i.e., $\dot{E}/V_R$ is about same for various H_S. Figure 10 shows the results of calculations for H_S = 3 m and u_L = 0.108 m·s^{-1}. Obviously three-phase fluidization is advantageous only for large solids diameter and small $\dot{E}/V_R$, i.e., small gas flow rates. For example, for 8 mm particles and $\dot{E}/V_R$ = 0.3 kW·m^{-3}, k_La''' is twice as high as in the two-phases system. Considering the higher driving force, the mass transfer per unit reactor volume could be even higher than by a factor of two.

Correlation for Small Particle Diameters ($d_S \leq 1$ mm)

Generally, the volumetric mass transfer coefficients k_La''' measured in gas-liquid fluidized beds depend on $\bar{u}_G$, u_L, and d_S (or terminal velocity of the solids which also depends on other solid and liquid properties that were kept about constant in this study). At same liquid velocity (e.g., u_L = 0.077 m·s^{-1}) applied for all particle sizes increasing the particle size from 0.05 to 8 mm, k_La''' passed a minimum at a diameter of 1–3 mm while ϵ_S steadily increased. At same particle size, increasing u_L increased the volumetric mass transfer coefficients and decreased ϵ_S. Thus k_La''' and ϵ_S were a function of d_S and u_L, whereas in the two-phase system no effect of liquid velocity on k_La was observed.

Plotting k_La''' against the solids fraction in the suspension ϕ_S:

$$\phi_S = \epsilon_S/(1 - \epsilon_G''') \quad (28)$$

All data for 0.05 mm $\leq d_S \leq$ 1 mm gave straight lines for various gas velocities (Figure 11). The data cover a twentyfold variation in particle diameter d_S and a twofold variation in liquid velocity u_L. It may thus be concluded that d_S and u_L merely determined the value of ϕ_S which can be used as the correlating parameter. The following relation was obtained by nonlinear regression analysis:

$$k_La''' = 0.39\left(1 - \frac{\phi_S}{0.58}\right)\bar{u}_G^{0.67} \quad (29)$$

(s^{-1}) ($m \cdot s^{-1}$)

($0.018\ m \cdot s^{-1} \leq \bar{u}_G \leq 0.16\ m \cdot s^{-1}$)

($0.05\ mm \leq d_s \leq 1\ mm$)

Equation 29 is based on 147 measurements in the air/water/glass spheres system that are described with 11% mean deviation. A parity plot is given in Figure 12. Additionally, the mass transfer

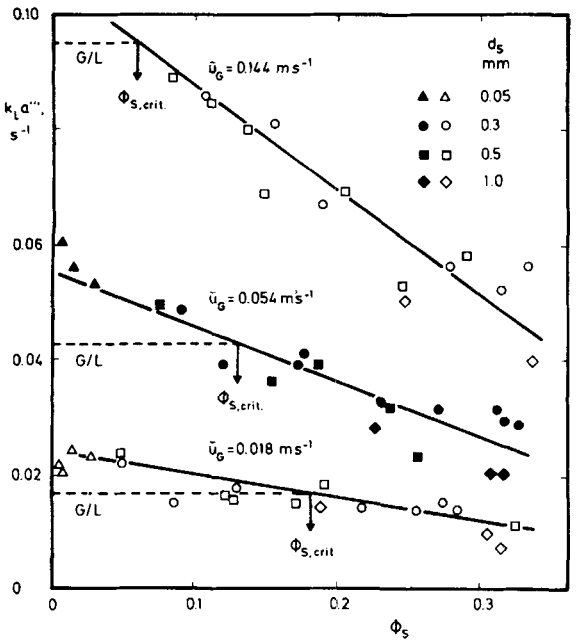

Figure 11. Dependence of $k_L a'''$ for 0.05–1 mm particles on solids fraction in the suspension.

coefficients for 1 mm glass balls determined by Østergaard and Fosbøl (1972) at bed heights $H_s > 1$ m are well described. (Information on phase holdups was taken from Michelsen and Østergaard, 1970.)

Obviously, the decrease of $k_L a'''$ with increasing solids loading is caused by the increase in suspension viscosity. Tentatively, the reciprocal of the term $(1 - \phi_S/0.58)$ can be interpreted as a measure of relative viscosity. An equation of the type

$$\frac{\mu_{SL}}{\mu_L} = \left(1 - \frac{\phi_S}{\phi_m}\right)^{-1} \tag{30}$$

has been used by Nicodemo et al. (1974) for correlation of the viscosities of glass spheres suspensions in aqueous polymer solutions. ϕ_m represents the solids fraction in the settled bed. According to Eq. 29, $\phi_m = 0.58$ is a reasonable value that is close to $\phi_m = 0.56$ fitted by Nicodemo et al. (1974). Accepting Eq. 29, $k_L a'''$ were inversely proportional to suspension viscosity. However, this cannot be unambiguously concluded from the present results since the suspension viscosities have not been measured.

Further investigations are needed for assessment of the influences of particle shape and density as well as different liquid properties. Particularly, increased liquid-side mass transfer coefficients k_L at low solid holdups cannot be expected from small and low-density solids that follow liquid motion. For the present data, by comparison of Eq. 29 and Eq. 25, the condition

$$\phi_S < 0.58 - 0.70\,\bar{u}_G^{0.15} = \phi_{S,\mathrm{crit}} \tag{31}$$

$$(\mathrm{m \cdot s^{-1}})$$

was obtained for solid loadings resulting in $k_L a$ increase as compared to the two-phase system. As is also evident from Figure 11, the limiting solids fraction $\phi_{S,\mathrm{crit}}$ decreases with increasing gas velocity. At very low solids loadings ($\phi_S < 0.01$), there has to be an increase of $k_L a'''$ with ϕ_S which has not been investigated. These effects deserve further study, preferably by separate determination of the different effects on k_L and a.

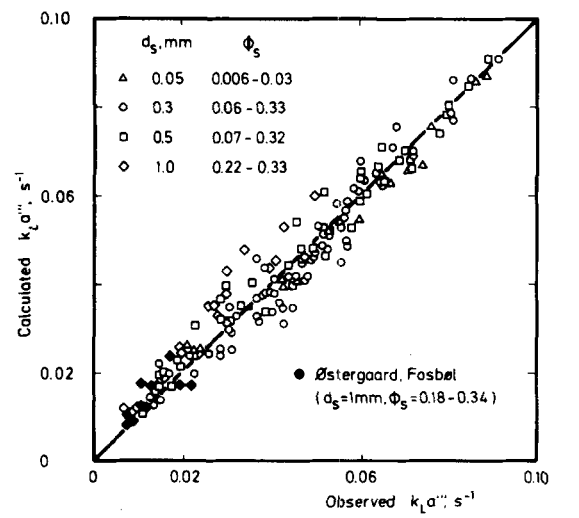

Figure 12. Parity plot for correlation of $k_L a'''$ in fluidized beds of 0.05–1 mm particles (Eq. 29).

ACKNOWLEDGMENT

Support from Deutsche Forschungsgemeinschaft is gratefully acknowledged.

NOTATION

- a = gas/liquid specific interfacial area with respect to reactor $(G/L/S)$ volume, $\mathrm{m^{-1}}$
- c = liquid-phase oxygen concentration, $\mathrm{kmol \cdot m^{-3}}$
- c^* = c in equilibrium to gas phase, $\mathrm{kmol \cdot m^{-3}}$
- c_o = c in liquid inlet stream, $\mathrm{kmol \cdot m^{-3}}$
- d_S = diameter of solid particles, mm
- D_C = bubble column diameter, m
- $\dot{E}$ = energy input, kW
- E_L = liquid-phase dispersion coefficient, $\mathrm{m^2 \cdot s^{-1}}$
- g = gravity acceleration, $\mathrm{m \cdot s^{-2}}$
- H_S = height of three-phase fluidized bed, m
- He = Henry's constant, $\mathrm{Pa \cdot m^3 \cdot kmol^{-1}}$
- j = cell number (BFCM-model)
- k = cell number of highest cell in three-phase zone
- k_L = liquid-side mass transfer coefficient, $\mathrm{m \cdot s^{-1}}$
- l = axial coordinate, m
- L = height of bubble column, m
- m_s = total mass of solids, kg
- $\dot{m}$ = mass flow rate, $\mathrm{kg \cdot s^{-1}}$
- N = total number of cells (BFCM model)
- $\dot{N}_G$ = molar flow rate of gas, $\mathrm{kmol \cdot s^{-1}}$
- P = pressure, Pa
- P_T = pressure at top of bubble column, Pa
- P_{TS} = pressure at top of three-phase zone, Pa
- Pe_L = liquid phase Peclet number defined in Eqs. 23 and 24
- R = gas constant, $\mathrm{kJ \cdot kmol^{-1} \cdot K^{-1}}$
- St = Stanton number defined in Eqs. 6 and 18
- T = temperature, K
- $\bar{u}_G$ = mean superficial gas velocity, $\mathrm{m \cdot s^{-1}}$
- u_L = superfical liquid velocity, $\mathrm{m \cdot s^{-1}}$
- V_R = reactor volume, $\mathrm{m^3}$
- x = dimensionless axial coordinate $(x(H_s) = 1)$
- y = gas-phase mole fraction of oxygen
- z = dimensionless axial coordinate $(z(L) = 1)$

Greek Letters

- α = parameter defined in Eqs. 9 and 10
- γ = backflow ratio (BFCM model) defined in Eqs. 21 and 22
- ϵ = relative holdup
- ρ = density, $\mathrm{kg \cdot m^{-3}}$
- ϕ_S = solids fraction in the suspension

Indices

- G = gas phase
- L = liquid phase
- mf = minimum fluidization
- o = gas or liquid entry at bottom of column
- S = solid phase

Superscripts

- $''$ = two-phase zone
- $'''$ = three-phase zone

LITERATURE CITED

Alvarez-Cuenza, M., and M. A. Nerenberg, "The Plug Flow Model for Mass Transfer in Three-Phase Fluidized Beds and Bubble Columns," *Cand. J. Chem. Eng.*, **59**, 739 (1981).

Dakshinamurthy, P., et al., "Studies of Gas-Liquid Mass Transfer in Gas-Liquid Fluidized Beds," *Fluidization and Its Applications*, H. Angelino et al., Eds., 429, Cepadues-Editions, Toulouse (1974).

Deckwer, W.-D., B. Burckhart, and G. Zoll, "Mixing and Mass Transfer in Tall Bubble Columns," *Chem. Eng. Sci.*, **29**, 2177 (1974).

Deckwer, W.-D., et al., "Oxygen Mass Transfer into Aerated CMC Solutions in a Bubble Column," *Biotechnol. Bioeng.*, **24**, 461 (1982).

Deckwer, W.-D., et al., "On the Applicability of the Axial Dispersion Model to Analyze Mass Transfer Measurements in Bubble Columns," *AIChE J.*, **29**, 915 (1983).

Dhanuka, V. R., and J. B. Stepanek, "Simultaneous Measurements of Interfacial Area and Mass Transfer Coefficients in Three-phase Fluidized Beds," *AIChE J.*, **26**, 1029 (1980).

Epstein, N., "Three-Phase Fluidization: Some Knowledge Gaps," *Canad. J. Chem. Eng.*, **59**, 649 (1981).

Henriksen, H. K., and K. Østergaard, "On the Mechanism of Break-up of Large Bubbles in Liquids and Three-Phase Fluidized Beds," *Chem. Eng. Sci.*, **29**, 626 (1974).

Lee, J. C., and H. Worthington, "Gas-Liquid Mass Transfer in Three-Phase Fluidized Beds," *Fluidization and Its Applications*, H. Angelino et al., Eds., 407, Cepadues-Editions, Toulouse (1974).

Michelsen, M. L., and K. Østergaard, "Hold-Up and Fluid Mixing in Gas-Liquid Fluidized Beds," *Chem. Eng. J.*, **1**, 37 (1970).

Nguyen-tien, K., "Gas-Flüssig Stoffaustausch im Dreiphasen-Wirbelbett," PhD Thesis, Universität Hannover (1984).

Nguyen-Tien, K., et al., "Liquid Dispersion in Three-Phase Fluidized Beds," *J. Chem. Eng. Japan*, **17**, 652 (1984).

Nicodemo, L., L. Nicolais, and R. F. Landel, "Shear Rate Dependent Viscosity of Suspensions in Newtonian and Non-Newtonian Liquids," *Chem. Eng. Sci.*, **29**, 729 (1974).

Østergaard, K., "Holdup, Mass Transfer, and Mixing in Three-Phase Fluidization," *Fluidization: Application to Coal Conversion Processes, AIChE Symp. Ser.*, **74**, No. 176, 82 (1978).

Østergaard, K., and P. Fosbøl, "Transfer of Oxygen Across the Gas-Liquid Interface in Gas-Liquid Fluidized Beds," *Chem. Eng. J.*, **3**, 105 (1972).

Østergaard, K., and W. Suchozebrski, "Gas-Liquid Mass Transfer in Gas-Liquid Fluidized Beds," Proc. Fourth Europ. Sympos. Chem. React. Eng., Brussels, 21 (1968).

Quicker, G., A. Schumpe, and W.-D. Deckwer, "Gas-Liquid Interfacial Areas in a Bubble Column with Suspended Solids," *Chem. Eng. Sci.*, **39**, 179 (1984).

Shah, Y. T., et al., "Design Parameters Estimations for Bubble Column Reactors," *AIChE J.*, **28**, 353 (1982).

Wen, C. Y., and Y. H. Yu, "Mechanics of Fluidization," *Fluid Particle Technology*, S. Lee, Ed., *Chem. Eng. Prog. Symp. Ser.*, **62**, No. 62, 100 (1966).

Manuscript received June 21, 1983; revision received Oct. 18 and accepted Oct. 20.

Removal of Colloidal Particles in Electroflotation

The collection mechanism of polystyrene latices of 0.6 μm in diameter in electroflotation has been examined both theoretically and experimentally as extension of our previous work (1980). To avoid the change of surface state of particle and bubble, the experiment was conducted under the condition that the concentration of CTAB (cetyl trimethylammonium bromide), cationic surfactant in the solution, is within the 90% of its initial concentration. It is of interest that the theory predicts the collection efficiency to vary as $d_i^{-1.91}$.

YOSHIHIRO FUKUI and SHINICHI YUU

Laboratory of Particle Mechanics
Kyushu Institute of Technology
Tobata Kitakyushu 804, Japan

SCOPE

The removal of suspended substances from effluents is important in waste water treatment from the environmental viewpoint. The particles to be removed in effluent treatment are normally less than about 20 μm and close to neutral buoyancy, and the concentration is also very dilute as low as 20 ppm.

Since it has been found effective empirically, to use very small bubbles often less than 100 μm in dia. for the removal of fine particles, electroflotation has become of interest. The diameter of bubbles generated by electrolysis is around 20 μm. This method is also advantageous, compared with the usual treatment technique in many aspects.

1) The apparatus is small and compact.

2) The system can be controlled electrically corresponding to the amount of floc.

3) The temperature of waste water does not affect the generation of gas bubbles even when it is high.

The electroflotation has been first applied to the treatment of domestic sewage in 1911 in the U.S. (Siegerman, 1971). At that time, however, because the electrodes tended to scum and scale stuck on the surfaces of the electrodes, the device prevented electric current from flowing. In Japan, several companies recently have solved these problems by developing their system in actual effluent treatment.

Though the actual system has been developed as noted above, the theoretical study of electroflotation itself has not been widely developed. The objective of this paper is to get information both theoretically and experimentally on collection mechanism which is of importance for the planning of actual apparatus.

In the recent study of flotation, Flint and Howarth (1971) calculated the collision efficiencies relating to a 6 μm galena particle and air bubble of diameter between 50 and 100 μm from limiting trajectories. Reay and Ratcliff (1975) have reported that the rate of flotation of glass beads varied approximately as the 1.5 power of particle diameter. They have suggested that the most fruitful course for future work would appear to be a series of experiments aimed at discovering how the flotation rate vs. particle size relationship depends on the zeta potential of the particles. Collins and Jameson (1976) have revealed that the rate